 Nucleic Acids Research, 1999, Vol. 27, No. 24 **4801–4806**

Thermal stability of PNA/DNA and DNA/DNA duplexes by differential scanning calorimetry

Munna C. Chakrabarti and Frederick P. Schwarz*

Center for Advanced Research in Biotechnology/National Institute of Standards and Technology, 9600 Gudelsky Drive, Rockville, MD 20850, USA

Received July 23, 1999; Revised and Accepted October 26, 1999

ABSTRACT

Thermodynamics of the thermal dissociation transitions of 10 bp PNA/DNA duplexes and their corresponding DNA/DNA duplexes in 10 mM sodium phosphate buffer (pH 7.0) were determined from differential scanning calorimetry (DSC) measurements. The PNA/DNA transition temperatures ranged from 329 to 343 K and the calorimetric transition enthalpies ranged from 209 ± 6 to 283 ± 37 kJ mol^{-1}. The corresponding DNA/DNA transition temperatures were 7–20 K lower and the transition enthalpies ranged from 72 ± 29 to 236 ± 24 kJ mol^{-1}. Agreement between the DSC and UV monitored melting (UVM) determined transition enthalpies validated analyzing the UVM transitions in terms of a two-state transition model. The transitions exhibited reversibility and were analyzed in terms of an AB = A + B two-state transition model which yielded van't Hoff enthalpies in agreement with the transition enthalpies. Extrapolation of the transition enthalpies and free energy changes to ambient temperatures yielded more negative values than those determined directly from isothermal titration calorimetry measurements on formation of the duplexes. This discrepancy was attributed to thermodynamic differences in the single-strand structures at ambient and at the transition temperatures, as indicated by UVM measurements on single DNA and PNA strands.

INTRODUCTION

Peptide nucleic acids (PNA) and DNA are analogs where the four nucleotides, adenine (A), thymine (T), guanine (G), and cytosine (C), are attached to an *N*-(2-aminoethyl)glycine backbone in the PNA sequence instead of the negatively charged deoxyribose phosphate backbone in DNA (1–4). UV monitored melting (UVM) studies of PNA hybrid duplexes in solution have shown that the PNA sequences can bind to their complementary single-strand DNA (5), RNA (6), and PNA (7) sequences with greater affinities than to their corresponding DNA sequences. However, in a previous paper (8) it was found that extrapolation of the UVM determined binding affinities and enthalpies of 10mer DNA/DNA and PNA/DNA duplexes to ambient temperatures did not yield the same binding affinities and enthalpies determined directly from isothermal titration calorimetry (ITC) measurements on formation of the duplexes. It was tentatively assumed that the two-state transition model analysis of the UVM results was correct and that this discrepancy was attributable to thermodynamic differences between the single-strand states at the duplex melting temperature and at ambient temperature as implied in an earlier study on PNA/DNA duplexes (9).

DNA/DNA binding thermodynamic quantities have also been determined from differential scanning calorimetry (DSC) measurements on the thermal dissociation or 'melting' of DNA/DNA duplexes at high temperatures (10–12). DSC measurements on the heat absorbed in the transition from a duplex to the single-strand states yield direct determinations of the binding enthalpy that are model-independent and direct determinations of the heat capacity change for the transition. Model-independent determinations of the enthalpy and heat capacity changes from DSC measurements on dissociation of the DNA/DNA and PNA/DNA duplexes would provide an additional independent method of determining DNA/DNA and PNA/DNA thermodynamic binding quantities. Furthermore, if extrapolation of these DSC values to ambient temperature yields enthalpy values which do not agree with the ITC results, then this implies that the thermodynamic single-strand states at ambient temperature are different than their presumably random coil states at the melting transition temperature. This was indeed observed in a UVM and DSC study of the melting of a 13mer DNA/DNA duplex where DSC scans on one of the single strands exhibited a conformational transition for the strand at a temperature well below the duplex melting temperature (12). An earlier comparison of the melting of 10mer and longer DNA/DNA duplexes showed that thermodynamic quantities determined from UVM measurements differed substantially from their values determined from DSC scans because the UVM results were incorrectly analyzed in terms of a two-state transition model and melting of the duplex was a multistate process (11). Thus, DNA/DNA and PNA/DNA melting temperatures determined from UVM measurements may not yield reliable estimates of the binding affinities at ambient temperature.

In this investigation, the thermodynamic quantities describing the melting or dissociation of PNA/DNA duplexes and their corresponding DNA/DNA duplexes were determined from DSC measurements. The thermodynamic quantities are the temperature at half the transition peak area (T_m), the ratio of

*To whom correspondence should be addressed. Tel: +1 301 738 6219; Fax: +1 301 738 6255; Email: fred@carb.nist.gov

the peak area to the number of moles of duplex in the sample or the calorimetric enthalpy (ΔH_c), the heat capacity change accompanying the transition (ΔC_p) from the difference in the post- and pre-transitional baselines at T_m, and the van't Hoff enthalpy (ΔH_v) from the shape of the transition peak. The duplexes consisted of the 10 bp sequences

H-ATGCXYATGC-$CONH_2$
3′-TACGX′Y′TACG-5′

for the PNA/DNA duplex and

5′-ATGCXYATGC-3′
3′-TACGX′Y′TACG-5′

for the corresponding DNA/DNA duplex where XY = TG, TC, AA, AG, CC, CG and X′Y′ are the complementary bases to XY in 10 mM sodium phosphate buffer, pH 7.0, containing 100 mM sodium chloride and 0.1 mM EDTA. The sequences will be referred to as PNA(XY) and DNA(XY) and the duplexes as PNA(XY)/DNA and DNA(XY)/DNA. These quantities are extrapolated to ambient temperature and compared to the binding free energy change, the binding enthalpy, and binding entropy determined from formation of the duplex in ITC measurements (8). UVM measurements were performed on single PNA strands to determine if indeed part of the discrepancies between the DSC and ITC measurements result from changes in the thermodynamic state of the single PNA strand states in going from ambient temperature to the duplex melting temperature.

MATERIALS AND METHODS

Materials

Single-strand PNA sequences were purchased from PE Biosystems (Framingham, MA) at a purity level >90% (m/m) as determined by HPLC and MALDI-TOF analysis. DNA sequences were synthesized and purified by Oligos Etc. Inc. (Wilsonville, OR) and were >90% (m/m) pure as determined by ion exchange HPLC and gel electrophoresis. Both oligomers (PNA and DNA) were dissolved in 10 mM sodium phosphate buffer, pH 7.0, containing 100 mM sodium chloride and 0.1 mM EDTA. Those reagents were purchased from Sigma Chemical Co. (St Louis, MO) and were reagent grade. The concentrations of the single-strand solutions were determined by UV absorption spectroscopy at 260 nm, using a Perkin Elmer Lambda 4B UV/VIS spectrophotometer and the extinction coefficients described previously (8). The duplexes were formed for ITC measurements using a Microcal Inc. Omega ITC where the single-strand DNA was titrated into the single complementary strand of PNA or DNA solution until saturation was obtained (8). The total strand concentration (C_t) was determined from the optical density (OD) at 260 nm divided by an extinction coefficient consisting of the sum of the single-strand DNA and single-strand PNA extinction coefficients divided by 2. The concentration of the duplex was taken as $0.5C_t$. The slight excess at most of ~5% of the DNA single-strand titrant divided by 2 is less than the error of 3% in each of the extinction coefficients so the slight excess was not considered in the calculation of C_t.

DSC measurements

DSC measurements were performed using a VP-DSC Microcalorimeter from Microcal Inc. (Northampton, MA). The DSC consists of a matched pair of 0.511 ml sample and reference cells. In a series of DSC scans, both cells were first loaded with buffer solution, equilibrated at 293 K for 15 min, and scanned from 20 to 90°C at a scan rate of 60 K/h. The buffer versus buffer scan was repeated once and upon the second cooling, the sample cell was emptied, rinsed, and loaded with the duplex solution prior to the 15 min equilibration period. This procedure was repeated for the other duplex solutions after each solution sample was scanned twice to check for reversibility. The sample solutions were from 0.02 to 0.05 mM duplex concentration and care was taken to minimize the presence of air bubbles in loading of the sample cell. The data were recorded every 2 s. After completion of a series of DSC scans, the second buffer versus buffer scan was used as the baseline scan and subtracted from the duplex versus buffer scans prior to analysis. The net DSC scan was analyzed for thermodynamic parameters using the EXAM software program (13). The pre- and post-transitional baselines were determined from least squares fits of straight lines to the data points, respectively, below the onset of the transition peak and following the return of the transition peak to the baseline. A sigmoidal baseline was determined under the transition peak by extrapolating the pre- and post-transitional baselines and employing the profile of the transition peak (13). The difference in the extrapolated baselines at the transition temperature divided by the number of moles of duplex is the heat capacity change. A two-state AB = A + B transition model was used to obtain ΔH_v for the transition. Values for ΔH_c were determined from the ratio of the transition peak area to number of moles of duplex and for ΔC_p were determined from the difference between the extrapolated pre- and post-transitional baselines at T_m. T_m was the temperature at half the peak area. The free energy change at the transition temperature or melting temperature, $\Delta G_b°(T_m)$, is

$$\Delta G_b°(T_m) = -RT_m\ln\{4/C_t\} \quad \mathbf{1}$$

where R is the gas constant 8.31451 J mol^{-1} K^{-1} (14). The heat of binding at the transition temperature, $\Delta H_b°(T_m)$, is then $-\Delta H_c(T_m)$ and as a function of temperature is

$$\Delta H_b°(T) = -\Delta H_c(T) = -\Delta H_c(T_m) - \Delta C_p(T - T_m) \quad \mathbf{2}$$

Thus, the free energy change for binding as a function of temperature is

$$\Delta G_b°(T) = T\Delta G_b°(T_m)/T_m - \{\Delta H_c(T_m) - \Delta C_p T_m\}\{[1 - T/T_m\} + T\Delta C_p \ln(T/T_m) \quad \mathbf{3}$$

It should be emphasized that the parameters of $\Delta H_c(T)$ and ΔC_p are model-independent, while $\Delta G_b°(T_m)$ assumes a two-state transition model. Finally, the change in the binding entropy as a function of temperature, $\Delta S_b°(T)$, is simply

$$\Delta S_b°(T) = \{\Delta H_c(T) - \Delta G_b°(T)\}/T \quad \mathbf{4}$$

To differentiate between the ITC determined values and the DSC values extrapolated to the ITC temperature, the notation

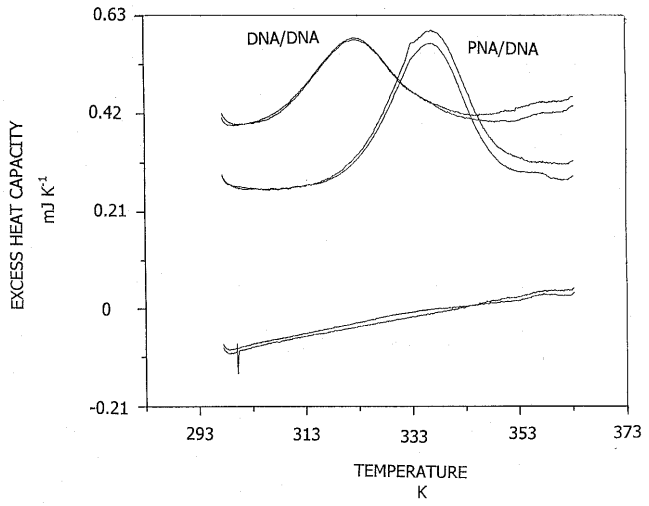

Figure 1. DSC scans of a 0.0344 mM PNA(TG)/DNA duplex solution, a 0.0303 mM DNA(TG)/DNA duplex solution, and the buffer (10 mM sodium phosphate buffer, pH 7.0, containing 100 mM sodium chloride and 0.1 mM EDTA) along with their repeated scans. The scan rate was 60 K h^{-1} and the cell volume was 0.511 ml.

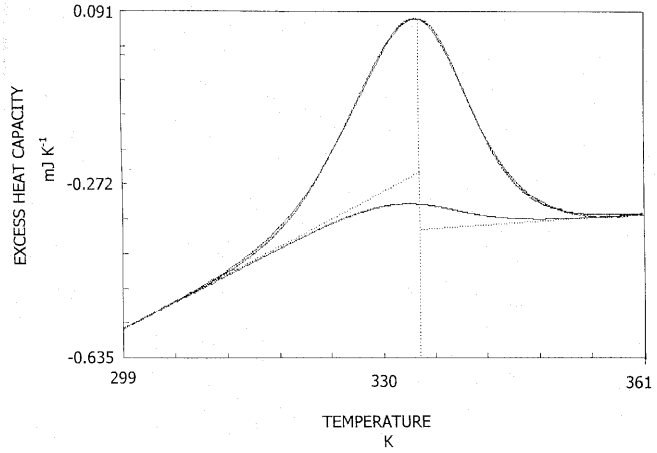

Figure 2. A DSC scan of a 0.0602 mM PNA(TC)/DNA duplex solution at a scan rate of 60 K h^{-1} in a cell volume of 0.511 ml. The fit of a two-state AB = A + B transition model to the DSC data is also shown on the plot by the broken lines.

of $\Delta H_b°$ (DSC) and $\Delta G_b°$ (DSC) will be used for the extrapolated DSC values and $\Delta H_b°$ (ITC) and $\Delta G_b°$ (ITC) for the corresponding ITC values from the literature. Thus, in equation **3** $\Delta G_b°(T) = \Delta G_b°$ (DSC) and in equation **2** $-\Delta H_c(T) = \Delta H_b°$ (DSC) at the ITC temperature T.

The uncertainties in the values of T_m, ΔH_c, $\Delta G_b°$, ΔH_v, and ΔC_p determined from several DSC scans of the duplexes represent only random errors inherent in the DSC measurements. There are also possible systematic errors which are combined in quadrature with these random errors to obtain a combined standard uncertainty for the final reported values of T_m, ΔH_c, $\Delta G_b°$, ΔH_v, and ΔC_p. Estimates of these systematic standard uncertainties are 0.1 K for T_m and 0.005 ΔH_v resulting from uncertainty in the calibration of the DSC power and temperature, 0.08 kJ mol^{-1} for $\Delta G_b°$, resulting from 3% uncertainty in the concentration determination, 0.03 ΔH_c and 0.03 ΔC_p resulting from uncertainty in the concentration determination and the DSC power calibration.

UVM measurements

The temperature dependence of the optical densities of the single PNA(TG) and PNA(TC) strands in solution were monitored at 260 nm by a Perkin Elmer Lambda 4B spectrophotometer equipped with a PTP-1 Peltier system for temperature scanning. The UV absorption cell containing the sample was heated at a rate of 1 K min^{-1} while the reference cell containing just the buffer solution was maintained at room temperature. The resulting increase in the optical density of the sample solution was recorded every 30 s over the temperature range 287–363 K. The temperature dependence of the hyperchromicity of the single DNA strands was less than that for the PNA strands. Changes in the hypochromicity of the single-strand solutions were analyzed by EXAM (13), which normalized the optical densities to the total optical density change and fitted the normalized data to a two-state A = B transition model. The extent of change in state of the strand, $\alpha(T)$, is, thus, the normalized optical density at temperature T. The temperature at the midpoint of the transition where $\alpha(T_m) = 0.5$ is the transition temperature T_m and the van't Hoff enthalpy for the transition, ΔH_v, is

$$\Delta H_v = 4R(T_m)^2 d\alpha(T_m)/dT \quad \textbf{5}$$

where $d\alpha(T_m)/dT$ is the slope of the normalized optical density versus temperature curve at T_m. Since for a two-state A = B transition, $\Delta G°(T_m) = 0$, the free energy change for the transition at 297 K, $\Delta G°$(297 K), is

$$\Delta G°(297\ \text{K}) = \Delta H_v(1 - 297/T_m) \quad \textbf{6}$$

There is a random uncertainty in the optical density measurements which was determined from several UVM scans of the sample and estimated systematic uncertainties of 0.003 ΔH_v from uncertainty in the temperature of the sample (0.1 K), and of 0.001 ΔH_v from uncertainty in the optical density reading. The random and estimated systematic uncertainties were combined in a quadrature to yield a combined standard uncertainty in the values for ΔH_v and $\Delta G°$(297 K).

RESULTS

Typical DSC scans of a 0.0344 mM PNA(TG)/DNA duplex solution, a 0.0303 mM DNA(TG)/DNA duplex solution, and the buffer are shown in Figure 1, along with their repeated scans. The peak maximum of the PNA(TG)/DNA duplex is shifted to a temperature almost 20 K higher than the peak maximum of the DNA(TG)/DNA duplex, indicating that the PNA/DNA duplex is more thermally stable than the corresponding DNA/DNA duplex. Also, the reappearance of the transition peaks upon a re-scan of the samples shows that the transitions are reversible and that there is no degradation of the sample after heating to 363 K. The results of applying a two-state AB = A + B transition model to the PNA(TC)/DNA data are shown in Figure 2.

Similar results were obtained for the other PNA/DNA duplexes and their corresponding DNA/DNA duplexes. The

Table 1. Thermodynamic quantities at the transition temperature from DSC measurements on the melting transitions of PNA/DNA and DNA/DNA duplexes

Duplex	Concentration (mM)	T_m (K)	ΔH_c (kJ mol^{-1})	$-\Delta G_b°$ (kJ mol^{-1})	ΔH_v (kJ mol^{-1})	$\Delta H_c/\Delta H_v$	$-\Delta C_p$ (J mol^{-1} K^{-1})
PNA(TG)/DNA	0.0344	335.9 ± 0.2	283 ± 37	30.6 ± 0.02	325 ± 11	0.86 ± 0.20	0
PNA(TG)/DNA[a]	0.0170	328.9 ± 0.1	246 ± 25	33.8 ± 0.1	230 ± 12	1.06 ± 0.20	559 ± 56
PNA(TG)/DNA[a]	0.0087	329.0 ± 0.1	255 ± 25	35.6 ± 0.1	259 ± 13	0.98 ± 0.20	652 ± 65
DNA(TG)/DNA	0.0316	323.2 ± 0.5	226 ± 21	29.7 ± 0.09	269 ± 15	0.84 ± 0.16	161 ± 26
PNA(TC)/DNA	0.0602	333.9 ± 0.6	233 ± 20	28.9 ± 0.05	310 ± 11	0.75 ± 0.16	115 ± 80
DNA(TC)/DNA[a]	0.0413	321.8 ± 0.1	236 ± 24	28.9 ± 0.1	280 ± 14	0.84 ± 0.16	30 ± 3
PNA(AA)/DNA	0.0309	330.1 ± 0.1	209 ± 6	29.5 ± 0.1	293 ± 3	0.72 ± 0.05	330 ± 11
DNA(AA)/DNA	0.0266	317.9 ± 0.8	136 ± 11	29.7 ± 0.08	284 ± 11	0.48 ± 0.20	0
PNA(AG)/DNA	0.0239	340.8 ± 0.2	272 ± 36	31.1 ± 0.1	325 ± 11	0.83 ± 0.19	447 ± 40
DNA(AG)/DNA[a]	0.0449	324.5 ± 0.1	206 ± 21	28.9 ± 0.1	300 ± 15	0.69 ± 0.13	131 ± 13
PNA(CC)/DNA[a]	0.0359	335.9 ± 0.2	227 ± 28	30.7 ± 0.1	351 ± 16	0.86 ± 0.17	0
DNA(CC)/DNA	0.0204	326.5 ± 0.8	72 ± 29	31.3 ± 0.07	379 ± 51	0.18 ± 0.17	0

[a]Results are from only one DSC scan so that the standard uncertainties are 10% for ΔH_c, 5% for ΔH_v, 20% for the ratio, and 10% for ΔC_p.

Table 2. Comparison at ambient temperatures between the thermodynamic quantities determined from the DSC measurements and the ITC measurements

Duplex	T (K)	$-\Delta G_b°$ (ITC)[a] (kJ mol^{-1})	$-\Delta G_b°$ (DSC) (kJ mol^{-1})	$-\Delta H_b°$ (ITC) (kJ mol^{-1})	$-\Delta H_b°$ (DSC) (kJ mol^{-1})	$-\delta(\Delta G_b°)$ (kJ mol^{-1})	$-\delta(\Delta H_b°)$ (kJ mol^{-1})	$\delta\Delta(S_b°)$ (J mol^{-1} K^{-1})
PNA(TG)/DNA	296.9	39.1 ± 0.2	61 ± 5	141 ± 4	283 ± 37	22 ± 5	142 ± 37	404 ± 126
DNA(TG)/DNA	296.9	37.4 ± 0.5	46 ± 2	178 ± 6	230 ± 22	9 ± 2	52 ± 23	145 ± 81
PNA(TC)/DNA	297.0	36.9 ± 0.6	52 ± 2	112 ± 7	237 ± 17	15 ± 2	125 ± 18	370 ± 61
DNA(TC)/DNA	296.7	38.4 ± 0.7	46 ± 2	176 ± 17	236 ± 24	7 ± 2	60 ± 29	178 ± 98
PNA(AA)/DNA	296.3	40.8 ± 0.3	48 ± 1	102 ± 6	220 ± 7	7 ± 1	118 ± 9	374 ± 30
DNA(AA)/DNA	298.1	36.1 ± 1.4	36.3 ± 0.9	204 ± 8	136 ± 11	0	68 ± 14	228 ± 47
PNA(AG)/DNA	296.0	42.6 ± 0.4	64.9 ± 0.7	102 ± 10	292 ± 36	22 ± 1	190 ± 37	568 ± 41
DNA(AG)/DNA	296.4	40.5 ± 0.3	44 ± 2	133 ± 6	210 ± 21	3 ± 2	77 ± 22	250 ± 75
PNA(CC)/DNA	296.4	39.3 ± 0.2	56 ± 3	150 ± 24	227 ± 28	17 ± 3	77 ± 37	202 ± 125
DNA(CC)/DNA	296.0	41.7 ± 1.3	33 ± 2	179 ± 8	72 ± 29	9 ± 2	102 ± 32	314 ± 108

[a]ITC values are from Schwarz *et al*. (8). The uncertainties are standardized uncertainties described in the text.

results in terms of the thermodynamic transition quantities, T_m, ΔH_c, ΔC_p, and ΔH_v are presented in Table 1. The transition quantities are the average values determined from analysis of several DSC scans of the same sample except for the lower PNA(TG)/DNA concentration samples, DNA(TC)/DNA, DNA(AG)/DNA, and PNA(CC)/DNA. The transition temperatures range from 328.9 K for PNA(TG)/DNA to 340.8 K for PNA(AG)/DNA for the PNA/DNA duplexes and from 317.9 K for DNA(AA)/DNA to 326.5 K for DNA(CC)/DNA. The calorimetric enthalpies range from 209 kJ mol^{-1} for PNA(AA)/DNA to 283 kJ mol^{-1} for PNA(TG)/DNA and from 72 kJ mol^{-1} for DNA(CC)/DNA to 236 kJ mol^{-1} for DNA(TC)/DNA. As observed previously (8), the PNA/DNA duplexes exhibit a dependence of the thermal stability on sequence. The ratio of the calorimetric enthalpies to the van't Hoff enthalpies determined from the AB = A + B two-state transition model is close to 1, except for DNA(CC)/DNA where the ratio is close to 0.2. It is not clear as to why the ratio is low for DNA(CC)/DNA. This shows that this model, as expected, accurately describes the PNA/DNA and DNA/DNA transitions as a two-state dissociation or melting of a duplex into two strands. The reduction in the transition temperature with reduction in the duplex concentration as exhibited by two out of the three different concentrations of the PNA(TG)/DNA duplexes (Table 1) also supports this two-state transition model.

The transition quantities and equations **2** and **3** were employed to extrapolate, respectively, the calorimetric enthalpies and the duplex melting free energy changes from the transition temperature to ambient temperature where ITC determinations of the binding quantities have been reported (8). Negative values of the extrapolated ΔH_c values were equated to the ITC binding enthalpies. The results of these extrapolations are presented in Table 2. The extrapolated DNA/DNA duplex quantities are in reasonable agreement with their ITC values since values within twice their standard uncertainties are considered the same. More specifically, the DNA/DNA $\delta(\Delta G_b°)$ values range from 0 to 9 ± 2 kJ mol^{-1} and the $\delta(\Delta H_b°)$ values from 52 ± 23 to 107 ± 30 kJ mol^{-1}. The extrapolated PNA/DNA transition quantities are also more negative than their ITC values. The discrepancies are quite large and range from 7 ± 1 to 22 ± 5 kJ mol^{-1} for $\delta(\Delta G_b°)$ and from 77 ± 37 to 142 ± 37 kJ mol^{-1} for $\delta(\Delta H_b°)$.

Table 3. Comparison at ambient temperatures between the thermodynamic quantities determined from the DSC and UVM measurements

Duplex	T (K)	$-\Delta G_b^\circ$ (UVM)[a] (kJ mol^{-1})	$-\Delta G_b^\circ$ (DSC) (kJ mol^{-1})	$-\Delta H_b^\circ$ (UVM) (kJ mol^{-1})	$-\Delta H_b^\circ$ (DSC) (kJ mol^{-1})	$-\delta(\Delta G_b^\circ)$ (kJ mol^{-1})	$-\delta(\Delta H_b^\circ)$ (kJ mol^{-1})
PNA(TG)/DNA	296.9	55 ± 1	61 ± 5	223 ± 1 (217 ± 24)	283 ± 37	6 ± 5	82 ± 12
DNA(TG)/DNA	296.9	46.0 ± 0.7	47 ± 2	206 ± 11 (214 ± 24)	230 ± 22	1 ± 2	24 ± 25
PNA(TC)/DNA	297.0	51.9 ± 0.5	52 ± 2	226 ± 12 (225 ± 3)	237 ± 17	0	11 ± 18
DNA(TC)/DNA	296.7	45.9 ± 0.5	46 ± 2	229 ± 10 (208 ± 10)	236 ± 24	0	7 ± 27
PNA(AA)/DNA	296.3	56.3 ± 0.7	49 ± 1	232 ± 12 (247 ± 7)	220 ± 7	7 ± 1	12 ± 14
DNA(AA)/DNA	298.1	42.2 ± 0.2	37.6 ± 0.9	192 ± 4	136 ± 11	4 ± 1	56 ± 12
PNA(AG)/DNA	296.0	66.7 ± 0.8	61.4 ± 0.7	267 ± 12 (298 ± 69)	292 ± 36	5 ± 1	25 ± 13
DNA(AG)/DNA	296.4	46 ± 2	46 ± 2	187 ± 2	210 ± 21	0	23 ± 22
PNA(CC)/DNA	296.4	51 ± 1	56 ± 3	254 ± 6	227 ± 28	5 ± 3	27 ± 25
DNA(CC)/DNA	296.0	56 ± 4	36 ± 2	267 ± 27 (224 ± 31)	72 ± 29	20 ± 4	195 ± 41

[a]UVM values are from Schwarz *et al.* (8). The uncertainties are standardized uncertainties as described in the text. The van't Hoff enthalpies in parentheses were determined from the slope of $1/T_m$ versus ln{OD} plots as described in Schwarz *et al.* (8).

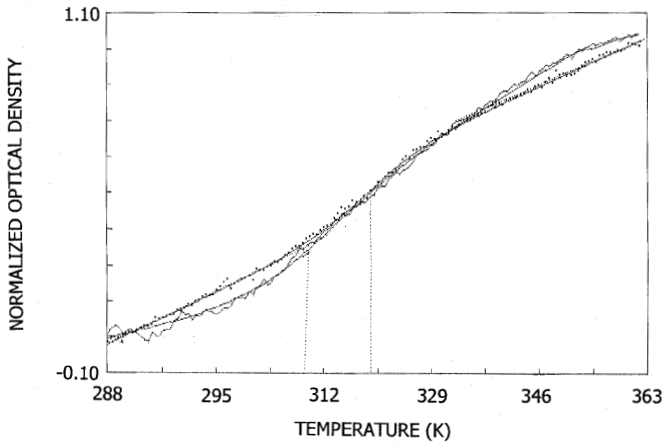

Figure 3. UVM curves of the single-strand DNA sequences. The dotted curve consists of the data points from a UVM scan of a 1.4 μM DNA(TG) solution and the continuous lower curve at 295 K consists of the data points from a UVM scan of a 1.5 μM DNA′(CA) solution. The smooth continuous line through each set of data points is the best least squares fit of a two-state A = B transition model to the data.

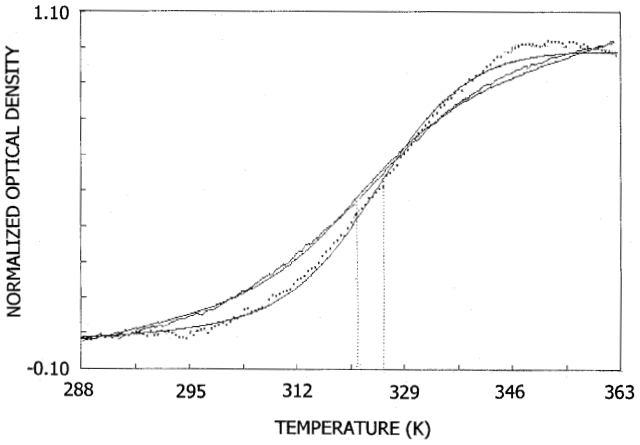

Figure 4. UVM curves of the single-strand PNA sequences. The broken curve consists of the data points from a UVM scan of a 0.37 μM PNA(TC) solution and the continuous upper curve at 295 K consists of the data points from a UVM scan of a 1.0 μM PNA(CC) solution. The smooth continuous line through each set of data points is the best least squares fit of a two-state A = B transition model to the data.

The DSC extrapolated binding free energy changes are in good agreement with the binding free energy changes obtained from reported UVM measurements (8) on the duplexes, with the exception of DNA(CC)/DNA, as shown in Table 3. Also in Table 3, there is good agreement between the DSC calorimetric enthalpies and the van't Hoff enthalpies obtained from the UVM results with the exception of DNA(CC)/DNA. The UVM binding free energy changes were calculated via equations **1** and **3** while the ambient UVM binding enthalpies were taken as the negative of the van't Hoff enthalpies at the transition temperature (8). This again verifies that the UVM results can be analyzed in terms of a two-state transition model.

Typical UVM scans of the melting of the single complementary DNA(TG) and DNA′(CA) strands are presented in Figure 3 and for the PNA(CC) and PNA(TC) strands in Figure 4. Average transition temperatures and van't Hoff enthalpies determined from two or more UVM scans on each strand over a concentration range from 0.2 to 2.0 μM are presented in Table 4, along with values for the two transitions exhibited by melting of the PNA(TG) strands. The low van't Hoff values indicate broad transitions, much broader than for the melting of the duplex transitions (Table 3) where the van't Hoff enthalpies are more than double their single-strand values in Table 4. The transition temperatures of the single strands, including the lower transition temperature of PNA(TG), are slightly lower than the melting temperature of the duplex containing the strand. This shows that the melting of the duplexes results in single-strand states that are different energetically than the single-strand states at ambient temperature. The transition temperatures and van't Hoff enthalpies are higher for melting of the single PNA strands than for the single DNA strands, indicating that the PNA single-strand states are more stable than the DNA single-strand states. This would account for the greater discrepancies between the ITC thermodynamic binding quantities and the extrapolated UVM

Table 4. Thermodynamic quantities at the transition temperature from UVM measurements on the melting transitions of DNA and PNA strands

Sequence	T_m (K)	ΔH_v (kJ mol^{-1})	$\Delta G°$ (297 K) (kJ mol^{-1})
DNA′(CA) GCATCAGCAT	318 ± 1	70 ± 3	4.6 ± 0.2
DNA(TG) ATGCTGATGC	320 ± 1	68 ± 4	4.9 ± 0.1
PNA(CC) ATGCCCATGC	325 ± 2	96 ± 6	8.3 ± 0.1
PNA(TC) ATGCTCATGC	329 ± 1	99 ± 9	9.6 ± 1.0
PNA(TG) ATGCTCATGC	302 ± 1	100 ± 10	1.7 ± 0.2
	336 ± 5	145 ± 32	

The uncertainties are standard uncertainties as described in the text.

thermodynamic quantities for the PNA/DNA duplexes than for the DNA/DNA duplexes.

DISCUSSION

The DSC results yield binding enthalpies (ΔH_c) for melting of the PNA/DNA and DNA/DNA duplexes that do not depend on the application of a specific transition model in the analysis of the results. Values for the enthalpies are also close to the van't Hoff enthalpies determined from UVM measurements on these duplexes, where a two-state transition model had been applied to the analysis of the data (8) and, thus, the analysis of the previous UVM results in terms of a two-state model for the duplexes is valid. Interestingly, for the DNA/DNA duplexes, the DSC and UV melting results yield extrapolated thermodynamic values closer to those determined directly from the ITC measurements than for the PNA/DNA duplexes. This was also observed by Ratilainen *et al*. (15) in a comparison of the formation and melting of 10 base lysine terminal PNA derivatives and their complementary DNA sequences. The larger discrepancies between the UVM extrapolated and ITC thermodynamic quantities at ambient temperature for the PNA/DNA duplexes than for the DNA/DNA duplexes are due to larger thermodynamic differences exhibited by the single PNA strand conformation at the melting and at ambient temperature. This is substantiated by the UVM measurements on the single PNA strands, which exhibit higher transition enthalpies than do the DNA strands as they are heated from 287 to 363 K. Furthermore, this conformation difference involves a change in the environment of the PNA and DNA bases, as evident from the increase in the hypochromicity at 260 nm from an interactive environment at low temperature to a more exposed environment at high temperature. Unpublished ITC results on the binding of PNA to complementary PNA strands exhibit broad titration peaks, which are indicative of slow binding reaction of the PNA to its complementary PNA sequence. This is most probably due to slow conformational changes in the PNA sequence upon binding to its complementary PNA sequence.

The thermodynamics of the single-strand transitions can contribute substantially to the differences between the extrapolated thermodynamic quantities from melting of the duplex and the ITC binding thermodynamic quantities at ambient temperature. For example, for the PNA(TG)/DNA duplex, the difference in the binding enthalpies between the ITC and the DSC measurements is –142 ± 37 kJ mol^{-1} and this is close to the sum of the van't Hoff enthalpies determined for the conformational change of the PNA(TG) strand (100 ± 10 kJ mol^{-1}) and for the conformational change of the complementary DNA′(CA) strand (70 ± 3 kJ mol^{-1}) in going from ambient to the duplex melting temperature. The smaller discrepancy in the extrapolated and ambient thermodynamic binding quantities exhibited by the DNA/DNA duplexes shows that the structure of the backbone plays an important role in the conformation of the oligonucleotide strand at ambient temperature. Detailed information on the structural changes of the more stable single PNA strands as the temperature is increased from ambient to above the melting temperature is being obtained from small angle neutron scattering measurements. More importantly, the results of this investigation show that the melting temperature of a PNA/DNA and a DNA/DNA duplex does not always yield a reliable estimate of the binding affinity of a PNA or a DNA to a complementary DNA sequence at ambient temperature. The assumption that structural changes in the single strands are negligible over the temperature range from ambient to the duplex melting temperature is not always correct.

ACKNOWLEDGEMENTS

This research was supported by NIST ATP Grant ATP99. Certain commercial equipment, instruments, and materials are identified in this paper in order to specify the experimental procedure as completely as possible. In no case does this identification imply a recommendation or endorsement by the National Institute of Standards and Technology, nor does it imply that the material, instrument, or equipment identified is necessarily the best available for the purpose.

REFERENCES

1. Nielson,P.E., Engholm,M., Berg,R.H. and Burchardt,O. (1991) *Science*, **254**, 1497–1500.
2. Egholm,M., Burchardt,O., Nielsen,P.E. and Berg,R.H. (1992) *J. Am. Chem. Soc.*, **114**, 1895–1897.
3. Harvey,J.C., Peffer,N.J., Bisi,J.E., Thomson,S.A., Cadilla,R., Josey,J.A., Ricca,D.J., Hassman,C.F., Bonham,M.A., Au,K.G., Carter,S.G., Brukstein,D.A., Boyd,A.L., Noble,S.A. and Babiss,L.E. (1992) *Science*, **258**, 1481–1485.
4. Buchardt,O., Egholm,M., Berg,R.H. and Nielsen,P.E. (1993) *Trends Biotechnol.*, **11**, 384–386.
5. Egholm,M., Buchardt,O., Christensen,L., Behrens,C., Freier,S.M., Driver,D.A., Berg,R.H., Kim,S.K., Norden,B. and Nielsen,P.E. (1993) *Nature*, **365**, 566–568.
6. Brown,S.C., Thomson,S.A., Veal,J.M. and Davis,D.G. (1994) *Science*, **265**, 777–780.
7. Wittung,P., Nielsen,P.E., Burchardt,O., Egholm,M. and Norden,B. (1994) *Nature*, **368**, 561–563.
8. Schwarz,F.P., Robinson,S. and Butler,J.M. (1999) *Nucleic Acids Res.*, **27**, 4792–4800.
9. Tomac,S., Sarkar,M., Ratilainen,T., Wittung,P., Nielsen,P.F., Norden,B. and Graslund,A. (1996) *J. Am. Chem. Soc.*, **24**, 5544–5552.
10. Albergo,D., Markey,L.A., Breslauer,K.J. and Turner,D.H. (1981) *Biochemistry*, **20**, 1409.
11. Breslauer,K. (1986) In Hinz,H.J. (ed.), *Thermodynamic Data for Biochemistry and Biotechnology*. Springer-Verlag, New York, NY, pp. 402–427.
12. Vesnaver,G. and Breslauer,K.J. (1991) *Proc. Natl Acad. Sci. USA*, **88**, 3569–3573.
13. Kirchhoff,W.H. (1993) *Exam: A Two-State Thermodynamic Analysis Program*, NIST Technical Note 1401. NIST, US Government Printing Office, Washington, DC, pp. 1–103.
14. Marky,L.A. and Breslauer,K.J. (1987) *Biopolymers*, **26**, 1601–1620.
15. Ratilainen,T., Holmen,A., Tuite,E., Haaima,G., Christensen,L., Nielsen,P.E. and Norden,B. (1998) *Biochemistry*, **37**, 12331–12342.